Applied Clay Science 53 (2011) 97–105

Contents lists available at ScienceDirect

Applied Clay Science

journal homepage: www.elsevier.com/locate/clay

Review Article

A review on characterization of pillared clays by specific techniques

Antonio Gil [a], Sophia A. Korili [a], Raquel Trujillano [b], Miguel Angel Vicente [b,*]

[a] Departamento de Química Aplicada, Universidad Pública de Navarra, Pamplona, Spain
[b] GIR-QUESCAT, Departamento de Química Inorgánica, Universidad de Salamanca, Spain

ARTICLE INFO

Article history:
Received 3 June 2010
Received in revised form 24 September 2010
Accepted 28 September 2010
Available online 13 October 2010

Keywords:
Pillared clays
Thermal Analysis
Near Infrared Spectroscopy
Ultraviolet–Visible Spectroscopy
Electron Paramagnetic Resonance
Mössbauer Spectroscopy

ABSTRACT

The use of specific characterization techniques, namely Thermal Analysis, Near Infrared Spectroscopy, Ultraviolet–Visible Spectroscopy, Electron Paramagnetic Resonance, Mössbauer Spectroscopy and Neutron Scattering, in the characterization of pillared clays is reviewed. Special emphasis is placed in the information provided by each of these techniques in the characterization of pillared clays.

© 2010 Elsevier B.V. All rights reserved.

1. Introduction

In recent years, Pillared InterLayered Clays (PILCs) have been widely used in several applications; in particular in adsorption and catalysis. Thus, the research interest in this family of solids has increased considerably. These solids are obtained from smectite clay minerals with the following three-step synthesis procedure: a) polymerization of a multivalent cation (such as Al^{3+}, Ga^{3+}, Ti^{4+}, Zr^{4+}, Fe^{3+}, and Cr^{3+}, among others), leading to polycations; b) intercalation of these polycations into the interlayer space of smectite clays, involving the substitution of natural exchangeable charge-compensating cations; and c) calcination at moderate temperatures. The latter step is necessary because the solids obtained after the second one, usually called *intercalated clays*, are metastable, like the polycations themselves. Calcination transforms the polycations into stable oxi-hydroxide phases named *pillars*, the solids obtained thus being called *pillared clays*.

Since polycations, and hence pillars, are voluminous, their insertion into the clay mineral layers involves layer separation to a long distance, while at the same time the clay mineral layers prevent the aggregation of the pillars during calcination, maintaining their dispersion. Thus, pillared clays show a characteristic porous structure, influenced by the number and size of the pillars in the interlayer region, which is in turn influenced by the cation exchange capacity of the original clay mineral and the charge of each individual polycation, among other factors. The intense research on PILCs carried out in the last decades means that more than one thousand references can be found in the literature, including several review articles and books reporting synthesis procedures, and the characterization and applications of these solids (only those published in the last decade are cited here as references: Gil et al., 2000, 2008, 2010; Ding et al., 2001; Serwicka and Bahranowski, 2004; Kloprogge et al., 2005; Bergaya et al., 2006).

Two techniques are by far the most widely used in the characterization of PILCs: X-ray diffraction and gas adsorption. The first provides immediate information about the success of the intercalation/pillaring process, evidenced by the shifting of the basal spacing to higher values; i.e. lower angles in the diffractograms. Moreover, such intercalation can be observed even faster by carrying out the diffraction of oriented films obtained by a single drop of suspension during synthesis. Nitrogen adsorption at −196 °C allows the estimation of specific surface area values, reported in almost all works in this field, and information about porosity by application of several models, reported to a lesser extent. These two techniques have been used to confirm the intercalation and pillaring processes. FT-Infrared (FTIR) and Nuclear Magnetic Resonance (NMR) spectroscopy are probably the next most widely used techniques used to characterize these materials. FTIR has been widely used to verify the pillaring process, describing the anchoring of the pillars to the clay mineral layer and cross-linking bonding, and also for analyzing the acid properties of these solids, mainly studied by pyridine adsorption. In the case of NMR, this allows study of the environment of ^{27}Al and ^{29}Si atoms in clays, and in the case of the solids pillared with Al-polycations it also allows the intercalating solutions, and the intercalated and pillared solids, to be studied, thus offering very interesting structural information.

Other techniques have been used to a much lesser extent; in some cases reported only in a few articles. Some of them can be used only

* Corresponding author. Tel.: +34 923294489; fax: +34 923294574.
E-mail address: mavicente@usal.es (M.A. Vicente).

0169-1317/$ – see front matter © 2010 Elsevier B.V. All rights reserved.
doi:10.1016/j.clay.2010.09.018

for a certain type of PILCs: i.e., visible spectroscopy is only applicable to PILCs containing transition elements, while temperature-programmed reduction can be applied to PILCs containing reducible cations (in both cases, only Fe- and Cr-PILCs can be studied). In other cases, the information provided by a given technique is very specific and such a technique might not be easily accessible, explaining its scant use in the study of these solids (e.g., Neutron Scattering). However, the information afforded by these specific techniques about the properties of pillared clays may be very interesting, and this is why we were prompted to review their usefulness for the study of these solids.

2. Specific techniques for characterization of pillared clays

As indicated earlier, besides the techniques most frequently used for the characterization of pillared clays – X-ray diffraction, nitrogen adsorption, infrared spectroscopy and nuclear magnetic resonance – many other techniques have been used, although to a lesser extent. Among them all types of techniques may be cited: spectroscopic techniques such as Ultraviolet–Visible, Near Infrared, Electron Paramagnetic Resonance or Mössbauer Spectroscopy; thermal techniques such as Thermogravimetry–Differential Thermal Analysis, Temperature Programmed Reduction, etc. Although an exhaustive review of all the studies carried out on pillared clays using these techniques is out of the scope of this short review, some relevant points of these studies are addressed in ensuing sections.

2.1. Ultraviolet–Visible Spectroscopy (UV–Vis)

As indicated, Fe^{3+} and Cr^{3+} are the only *d*-block elements used for the intercalation of pillared clays, and hence the only cations studied by visible spectroscopy. However, two important points should be noted before continuing. One is the fact that the UV–Vis region has been studied in some clay minerals, mainly in those pillared with Ti and Zr species, obtaining information from the Ultraviolet region (this information is not reviewed here). The second is that visible spectroscopy has also been used to study *doped* PILCs; that is, pillared clays into which small amounts of other element(s) have been incorporated by adding it (them) to the intercalating solution. The same is applicable when transition elements are incorporated by impregnation onto pillared-clay minerals. Although these solids are evidently very important, in a strict sense, the transition elements are not the constituents of pillaring solutions. Additionally, many elements have been incorporated in pillared clays, such as V, Cr, Mn, Co, Ni, Cu, Pd, Ag, and Pt, among others, and a review of these solids is beyond the scope of the present study. Thus, only the *true* pillared clays containing Cr- or Fe-polycations will be considered here.

In the case of Cr-PILCs, the polymerization of Cr^{3+}, and hence the nature of the intercalating species, can be monitored by visible spectroscopy. Polymerization of this cation leads to the formation of the dimer $[Cr_2(OH)_2(H_2O)_8]^{4+}$, the trimer $[Cr_3(OH)_4(H_2O)_9]^{5+}$, the tetramers $[Cr_4(OH)_6(H_2O)_{11}]^{6+}$ and $[Cr_4(OH)_5O(H_2O)_{10}]^{5+}$, and even of a pentameric and a hexameric polycation, hitherto not described in detail. The position of the two bands appearing in the visible spectra varies strongly: between 408–426 and 575–584 nm, depending on the degree of polymerization, the ratio between their extinction coefficients also varying between 1.17 and 1.60 (Finholt et al., 1981; Thompson and Connick, 1981; Stünzi and Marty, 1983; Spiccia and Marty, 1986; Spiccia et al., 1987, 1988). The nature of the polymeric species present in a given solution can be deduced by comparing the spectra with reported results.

Brindley and Yamanaka (1979) used these data to conclude that their intercalating solution may have been composed of the dimer $[Cr_2(OH)_2(H_2O)_8]^{4+}$, while Volzone et al. (1993) and Volzone (1995, 2001) described the change in color of the intercalating solution, obtaining peaks at 424 and 585 nm, although they did not discuss the composition of the solution in detail. Toranzo et al. (1997) and Mata et al. (2007) studied the polymerization process of a series of Al–Cr mixed solutions, from the Al alone- to the Cr alone-containing cases. Those authors reported that the degree of polymerization depended on the Al^{3+}/Cr^{3+} ratio, since the acidity of both cations elicits a strong competition by the OH^- added to the solution during the polymerization process. The formation of the trimer was found for the pure- and rich-chromium solutions, while the dimer, and even no polymerization of this cation, was found when the more acidic Al^{3+} was the major cation in the solution. The nature of the polycations once incorporated in the saponite clay may be different to that of the polycations in solution. It should be considered that the intercalating solutions are added to clay suspensions, which are slightly alkaline ($pH \approx 8$), which can alter the polymerization before the polycations enter the basal spacing.

Diffuse reflectance spectra of the intercalated solids reveal three well defined bands, close to 230, 420 and 590 nm, corresponding to the three spin-allowed transitions in Cr^{3+}, and a shoulder close to 690 nm, corresponding to the spin-forbidden ruby line (Fig. 1). The position of these bands changes, depending on the Cr^{3+}/Al^{3+} atomic ratio in the intercalating solution. The position of the bands also changes strongly under calcination, shifting to lower wavenumbers: that is, the crystal field stabilization energy and the Racah parameter also decrease. This allows a follow-up of the transformation from the polycations (fairly ionic, with hydroxyl groups and water molecules) to the covalent pillars, which are close to Cr_2O_3-eskolaite, as shown by the evolution of the β parameter, which is closer to 1.0 in the pillared solids (Table 1, Vicente et al., 1998).

The incorporation of iron to PILCs does not elicit such clear effects, since Fe^{3+} in the polycationic species does not have spin-allowed bands, owing to its d^5 configuration. Belver et al. (2004a) have reported the DR-UV–Vis spectra of mixed Al–Fe-PILCs prepared from saponite and solutions containing various Al/Fe ratios (Fig. 2). These spectra show a broad band with a maximum in the UV region, close to 300 nm, and a large shoulder at higher wavelengths, reaching the visible region and typical of the charge transference of Fe^{3+} in hydroxo-complex species. These patterns were similar for all Fe samples, and clearly differed from that of the Fe-free Al-PILC, which showed a narrower band in the UV region, also due to the charge transfer process. While calcining the intercalated solids, no changes in the spectra were observed, although the color of the samples changed from pale brown to dark brown or even black, the wide charge transference shoulder remaining almost unchanged.

2.2. Near Infrared Spectroscopy

Near Infrared (NIR) is the region of the electromagnetic radiation with a wavelength between 800 and 2500 nm and a wavenumber between 12,500 and 400 cm^{-1}, and it is the most energetic infrared region, close to the visible region. It has been much less used than the *usual* infrared radiation: between 4000 and 300 cm^{-1}. In fact, this spectroscopy is carried out on UV–Vis devices, not on IR apparatus. Overtones and combination bands are the effects observed by means of this spectroscopy.

NIR spectroscopy has been little used for the characterization of pillared clays. Vicente et al. reported the characterization of pillared Ballarat saponite (Vicente and Lambert, 1999, 2001; Vicente et al., 2004) with this technique. The overtone of the stretching vibration of the structural OH of the original saponite was found at 1389 nm, while the overtone of this vibration in water molecules was observed as two effects at 1408 and 1461 nm, suggesting the presence of two kinds of water molecule, as corroborated by the fact that these effects were not observed in the intercalated solid, in which a broad band was observed at this position. The $\nu + \delta$ combination band of water was reported at 1907 nm, while that from structural OHs appeared as

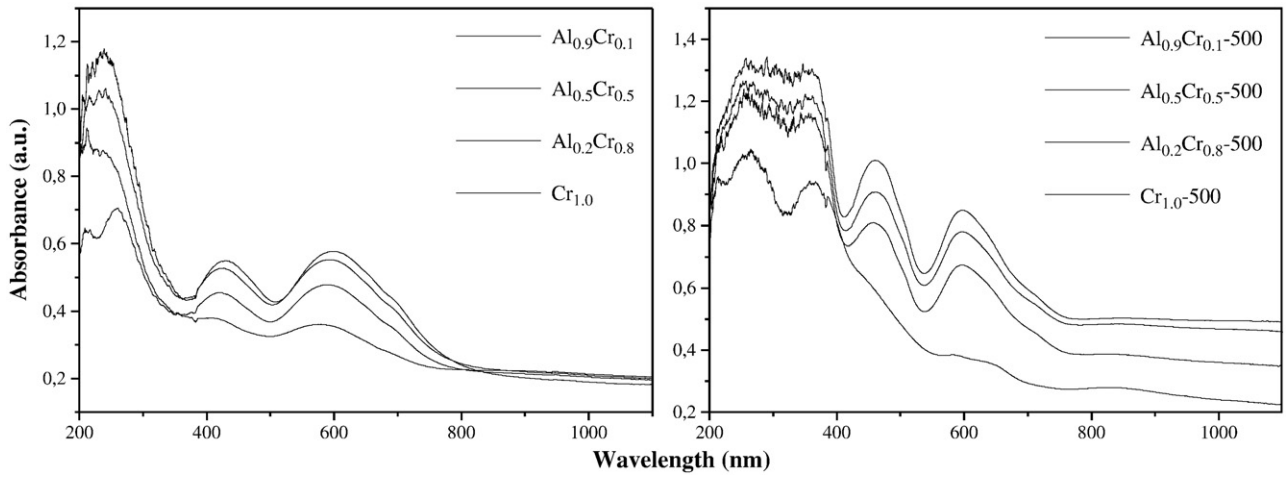

Fig. 1. Diffuse reflectance spectra of saponite treated with Al–Cr polycations, solids intercalated (left) and pillared by calcination at 500 °C (right). The subscripts under the name of the solids indicate the Al and Cr molar fractions.
Adapted from Applied Catalysis A: General, 327, G. Mata, R. Trujillano, M.A. Vicente, C. Belver, M. Fernández-García, S.A. Korili, A. Gil, Chromium-saponite clay catalysts: Preparation, characterization and catalytic performance in propene oxidation. Copyright (2007), with permission from Elsevier.

three bands between 2100 and 2400 nm (2210, 2318 and 2388 nm), depending on the precise environment of the OH groups.

Ballarat saponite has been subjected to pillaring with $[Al_{13}(\mu_3\text{-}OH)_6(\mu_2\text{-}OH)_{12}(heidi)_6(H_2O)_3]^{3+}$ (in short, Al_{13}-heidi), a polycation that contains the organic moiety called *heidi* [N-(2-hydroxyethyl)iminodiacetate anion]. In the region of the OH ($\nu+\delta$) combination band, a shoulder is present at 2250 nm, both in the intercalated (dried) and pillared (calcined at 500 °C) solids, which can be assigned to the bridging OHs in Al_{13}-heidi polycations, since in these polycations there are two types of hydroxyls (μ_2 and μ_3), different from those in the original saponite. The overtone of C–H stretching is found at c.a. 1725 nm in the intercalated solids, disappearing in the pillared ones, confirming the complete elimination of these groups under calcination, while the combination mode of these bonds, expected at c.a. 2300 nm, is not visible due to overlapping with M-OH vibrations (Fig. 3).

When these solids were impregnated with $[Pt(NH_3)_4]^{2+}$ complex, the overtone of NH bonds was observed at 1550 nm, indicating that some NH_3 ligands had remained in the impregnated solids, coordinating the Pt(II) cations. This band was still present when the impregnated solids were heated to 150 °C and completely disappeared after further heating to 250 °C. The heat treatment at the latter temperature resulted in the evolution of platinum species on the surface of the pillared-clay support. In the same way, the overtone of OHs from adsorbed water almost completely disappeared after heating at 150 °C, while the bands ascribed to structural OHs remained clearly observable.

This saponite, and also Yunclillos saponite and Gador montmorillonite, were submitted to pillaring with the classical Al_{13}-Keggin polycation, and then impregnated with metallic complexes; namely, acetylacetonate and ethylenediamine derivatives. It was observed that the region of structural OH groups was richer in the saponites than in the montmorillonite, in agreement with the different types of structural OHs. NIR also proved to be a useful tool to characterize the impregnated solids; analysis of the bands from the N–H and C–H bonds under heating allowed the decomposition of the impregnated precursors to be followed (Vicente et al., 2004).

2.3. Electron Paramagnetic Resonance (EPR)

This technique has been used by a few authors for the study of Fe- and Cr-PILCs. Belver et al. (2004b) used this technique to study in detail the Fe species produced by pillaring saponite with Al–Fe mixed polycations. The spectra showed two main signals: one centered at $g \approx 4.2$, with an axial shape and displaying a shoulder at $g \approx 9$, and the other at around $g \approx 2$, sometimes overlapped by a sextet produced by the very small amount of Mn^{2+} in the original clay mineral (Fig. 4). The signal at $g \approx 4.2$, with a shoulder at $g \approx 9$, was attributed to isolated octahedral Fe^{3+} species subject to a rhombic distortion, while the broad signal at $g \approx 2$ was ascribed to hydrated Fe^{3+} species, giving rise to microdomains of superparamagnetic nanosized particles as Fe_2O_3 or FeOOH. This was corroborated upon obtaining the spectra at

Table 1
Data from the diffuse reflectance spectra of Al–Cr intercalated and pillared saponite. The subscripts in the names of the samples indicate the Cr and Al molar fractions.
Adapted from Vicente et al., Anales de Química — International Edition, 1998.

	$Cr_{0.1}Al_{0.9}$		$Cr_{0.2}Al_{0.8}$		$Cr_{0.5}Al_{0.5}$			$Cr_{0.8}Al_{0.2}$		$Cr_{0.9}Al_{0.1}$		$Cr_{1.0}$		
	Interc.	Pill. 500	Interc.	Pill. 500	Interc.	Pill. 200	Pill. 500.	Interc	Pill. 200	Interc.	Pill. 200	Interc.	Pill. 200	Pill. 500
CT	39,100	38,500	39,200	37,900	43,500	41,700, 28,600	37,800, 28,600	41,700	38,400	41,700	39,200	43,100	39,200, 26,450	38,000, 28,700
ν_2	24,400	22,700	24,500	23,000	24,100	–	22,000	24,000	26,300	23,900	–	23,800	–	21,900
ν_1	17,600	16,800	17,500	16,800	17,100	17,100	16,800	16,900	–	16,950	–	16,900	–	16,800
ν_4	–	–	–	14,100	14,600	–	13,950	14,700	14,300	14,450	14,200	14,450	–	14,200
B	672	608	704	613	706	–	572	722	–	739	–	834	–	559
β	0.73	0.66	0.77	0.67	0.77	–	0.62	0.79	–	0.81	–	0.91	–	0.61

Interc. = intercalated samples (dried at 50 °C). Pill. X = pillared samples, calcined at X °C. CT = charge transference. B = Racah parameter. β = β parameter (β = B/Bo, Bo being Racah parameter of the free cation). CT, ν_2, ν_1, ν_4 and B, all in cm^{-1}.

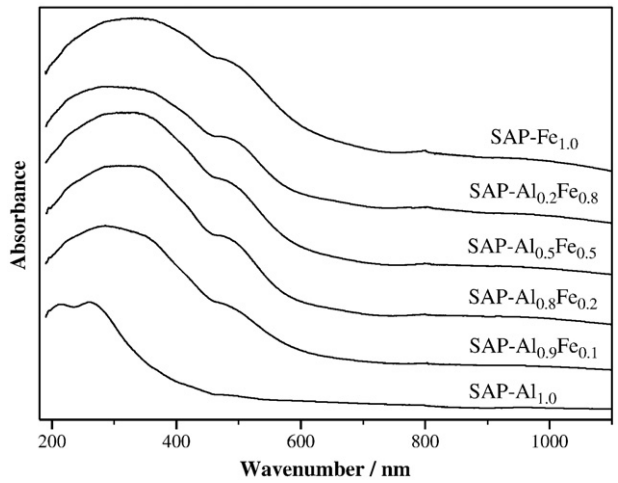

Fig. 2. UV–Vis spectra of Al–Fe intercalated saponite (the subscripts under the name of the solids indicate the Al and Fe molar fractions).
Reprinted from Applied Catalysis B: Environmental, 50, C. Belver, M.A. Bañares, M.A. Vicente, Fe-saponite pillared and impregnated catalysts. I. Preparation and characterisation. Copyright (2004), with permission from Elsevier.

room temperature: the signal at $g \approx 4.2$ and the shoulder at $g \approx 9$ decreased in intensity without lineshape change when the spectrum was recorded at room temperature, while the signal at $g \approx 2$ did not decrease its intensity upon increasing the temperature. Furthermore, a small shift of the signal towards higher magnetic fields with a certain decrease in the width and anisotropy of the signal was detected in the spectra recorded at room temperature. This behavior is typical of superparamagnetic or even ferromagnetic coupling between Fe^{3+} species. The signals were very similar for all samples, regardless of the iron content, indicating the presence of similar types of dispersed Fe species. However, the signal at $g \approx 2$ in the spectrum obtained at −196 °C from the solid pillared with pure Fe-polycations showed higher anisotropy and a different behavior with respect to the recording temperature. This suggested changes in the nuclearity of the Fe_2O_3 or FeOOH clusters, which may have been due to an increase in the size of the particles of these phases when the amount of Fe fixed during the pillaring procedure was increased. Quantification of the dispersed Fe species is difficult, and the presence of certain amounts

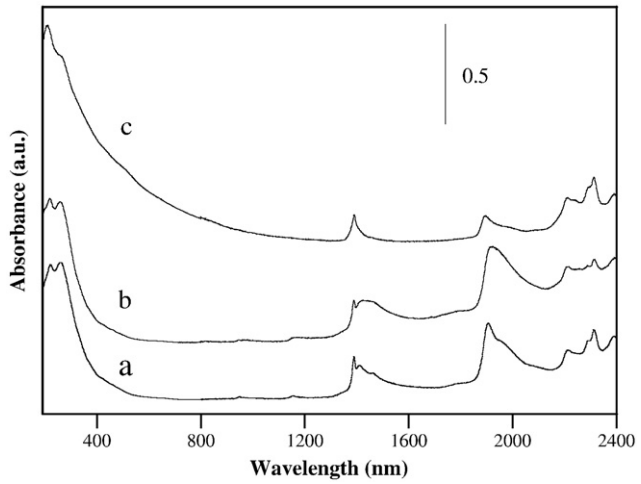

Fig. 3. NIR spectra of Ballarat saponite (a) and Al_{13}-heidi intercalated (b) and pillared (c) samples.
Reproduced by permission of the PCCP Owner Societies from Vicente and Lambert, 1999 (http://dx.doi.org/10.1039/a808291j).

of antiferromagnetically coupled phases (like α-Fe_2O_3), not detected by EPR, cannot be ruled out. The main conclusion is that EPR spectroscopy allows the similarity of Fe species to be seen in all the pillared solids.

Yunclillos saponite pillared with mixed Al–Cr polycations, with several Al/Cr ratios, has also been characterized by EPR measurements (Mata et al., 2007). The EPR spectra of chromium species on several oxide surfaces have been interpreted on the basis of three signals, denoted as γ, β and δ, respectively (Fig. 5). The axial γ-signal appears at a g-factor value of 1.9 and has been assigned to isolated Cr(V) species, while the β-signal is attributed to Cr_2O_3-like clusters and the δ-signal to isolated or dispersed Cr(III) species. In the Al–Cr pillared saponite, two signals are observed. The first one (denoted I in Fig. 5), centered at $g = 4.2$ with a shoulder at $g = 9$, was assigned to Fe^{3+} species with rhombic distortion, compatible with the presence of this cation in the octahedral layer of the clay. The second signal (denoted II in Fig. 5), a symmetrical line at $g = 1.97$, was compatible with bibliographic assignations to Cr(V) (γ signal), to Cr(III) as α-Cr_2O_3 (β signal), and also to a trimer of mixed valence: Cr^{6+}–Cr^{3+}–Cr^{6+} (γ signal). The spectra recorded at room temperature showed that the intensity of the second signal decreased when the annealing temperature was increased, a behavior characteristic of the transformation from paramagnetic to non-paramagnetic species, which is related to the weakly paramagnetic Cr_2O_3. Although EPR did not allow Cr(VI) species to be detected, its combination with other techniques confirmed the presence of Cr(III) and Cr(VI) species in all the pillared saponites.

2.4. Mössbauer Spectroscopy

Among pillared clays, this technique has been used for the characterization of Fe-PILCs and Sn-PILC. Bakas et al. (1994) carried out a ^{57}Fe Mössbauer study, between −268.9 and 19 °C, of a montmorillonite pillared with mixed Al–Fe (Al/Fe = 1). The spectra of the samples obtained by heating under an oxidizing atmosphere showed a dominant symmetric quadrupole doublet with hyperfine parameters, which corresponded to paramagnetic Fe^{3+} in octahedral coordination, while the spectra of the samples obtained by heating in a reducing atmosphere consisted of two paramagnetic components – one ferric and another ferrous, the doublet with higher intensity – and a weak magnetic component with hyperfine parameters corresponding to metallic Fe. The spectra obtained at −253 °C were very similar to those obtained at 19 °C. At −286.9 °C, the spectra of the intercalated solid and of the solid calcined under an oxygen atmosphere showed three ferric components: one paramagnetic (doublet) and two magnetic sextets. The area of the paramagnetic component was about 9% of the total spectral area; 90% at −253 °C, and 100% at 19 °C. In the case of the samples obtained under reducing conditions, their spectra at −268.8 °C required more than one ferrous and one ferric magnetically split components. The intercalating species was identified as lepidocrocite, which was transformed into Al-substituted maghemite by heating in air, and into Al-substituted magnetite when heating was carried out under a hydrogen atmosphere. The temperature dependence of the Mössbauer spectra showed that the size of the oxide particles was smaller than 10 nm. When the samples were subjected to reducing treatments, broken pillars were formed, which did not sinter under later oxidizing treatment regardless of the step of the synthesis in which the reduction was carried out. Cyclic redox heat treatments proved to be an effective method for changing the morphology of the inserted nanoparticles.

Stievano et al. (2006) have reported the intercalation of saponite with the polycation $[Fe_8(\mu_3\text{-}O)_2(\mu_2\text{-}OH)_{12}(tacn)_6]^{8+}$, in short Fe_8-tacn, where *tacn* is 1,4,7-triazacyclononane, the solids obtained being studied by ^{57}Fe Mössbauer Spectroscopy at −268.9 and 20 °C (Fig. 6). The spectrum of the pure Fe_8-tacn bromide salt displayed three main

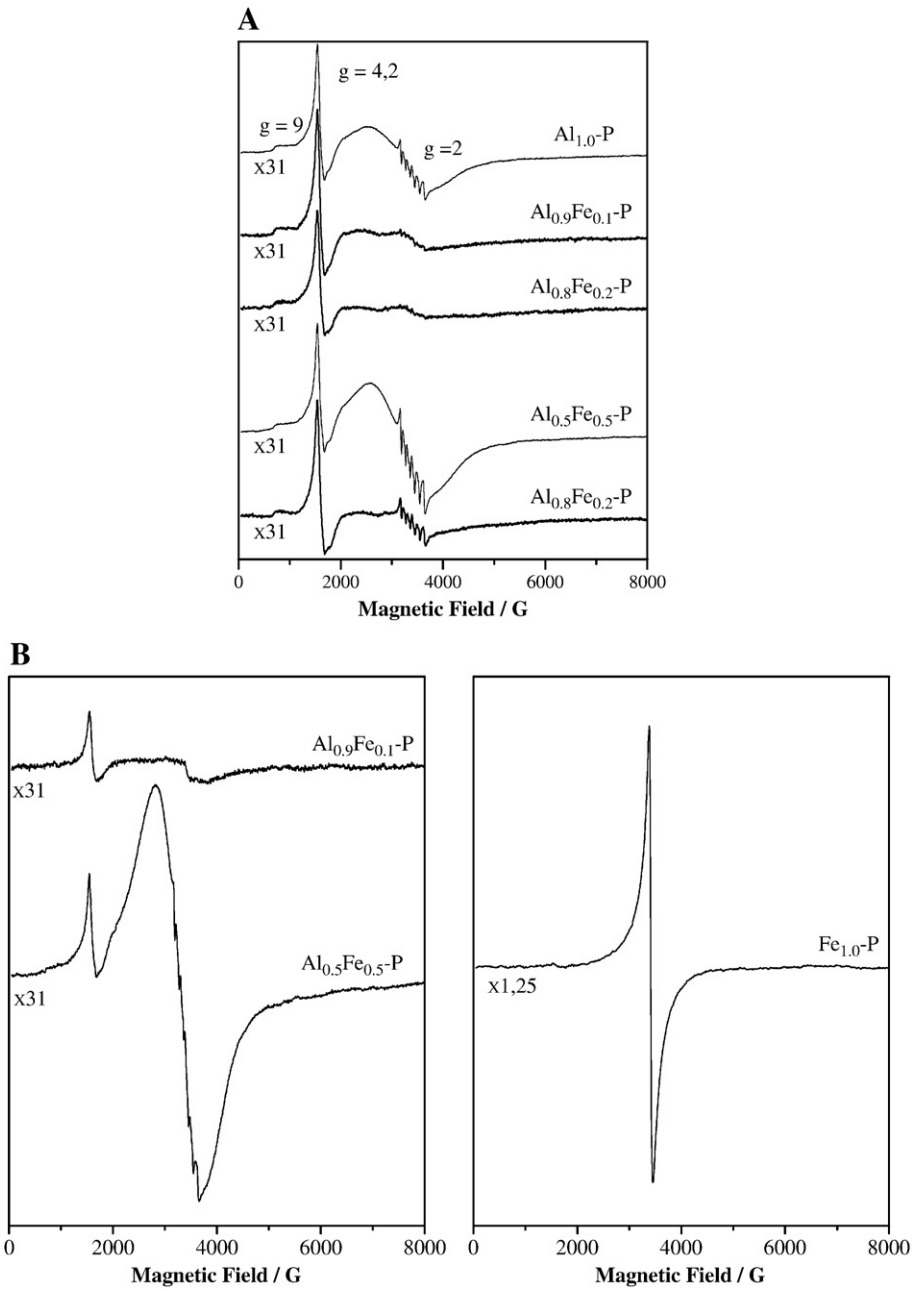

Fig. 4. (A) EPR spectra of Al–Fe pillared saponite recorded at −196 °C (A) and at 25 °C (B). The subscripts under the name of the solids indicate the Al and Fe molar fractions. Reprinted from Applied Catalysis B: Environmental, 50, C. Belver, M.A. Vicente, A. Martínez-Arias, M. Fernández-García, Fe-saponite pillared and impregnated catalysts. II. Nature of the iron species active for the reduction of NO_x with propene. Copyright (2004), with permission from Elsevier.

magnetic sextets with a relative intensity of 2:1:1, assigned to the three iron sites in the structure of the octamer; the eight Fe atoms of the octamer had relative abundances of 4:2:2. A small quadrupole doublet visible in the central region of the spectrum was assigned to the presence in the sample of small amounts of impurities (identified by the authors as "oxidic iron"). Similar results were obtained for a frozen aqueous solution of this compound, showing that the cation had retained its structure in solution, although the intensity of the quadrupole doublet in the central part of the spectrum was slightly more intense than in the solid salt, suggesting the decomposition of a minor part of the polycation, probably in solution.

The spectrum of pure saponite showed three main spectral components (Fig. 6). The first two components were quadrupole doublets with hyperfine parameters typical of divalent and trivalent iron in octahedral coordination, compatible with the occupation of the octahedral layer of saponite. The third component, which was less intense, was a magnetic sextet, probably related to highly dispersed paramagnetic iron species, also probably located in the octahedral layer of the saponite and undergoing slow spin relaxation at low temperature. The spectrum of the intercalated solid appeared as the sum of those of the clay mineral and the polycation, showing the two quadrupole doublets from the clay mineral and the three sextets of relative intensity 2:1:1 from the polycations. However, the hyperfine parameters of the magnetic sextets in the polycations showed small differences; they appeared at 52.3, 47.7 and 45.6 T in the pure polycations and at 50.1, 47.4 and 44.4 T in the intercalated species. These changes suggested a rearrangement of the structure of the cation in the interlayer space of the clay.

Petridis et al. (1989) carried out a ^{119}Sn Mössbauer study between −193 and 27 °C of a montmorillonite pillared with the trimeric species $[\{(CH_3)_2Sn\}_3(OH)_4]^{2+}$, obtained *in situ* by the polymerization

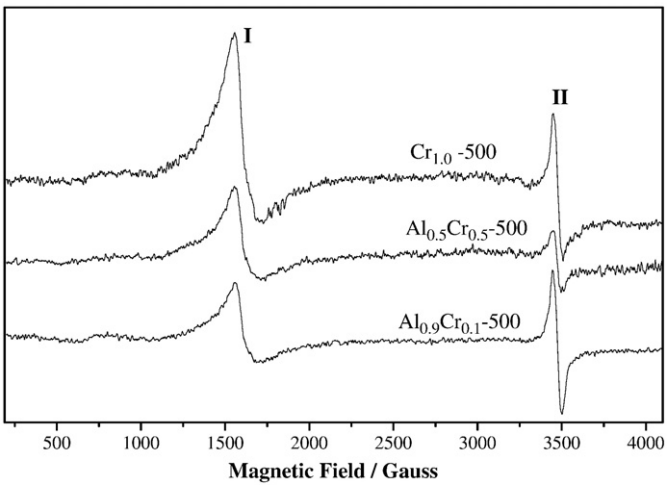

Fig. 5. EPR spectra of the solids indicated recorded at −196 °C after outgassing (the subscripts under the name of the solids indicate the Al and Cr molar fractions).
Reprinted from Applied Catalysis A: General, 327, G. Mata, R. Trujillano, M.A. Vicente, C. Belver, M. Fernández-García, S.A. Korili, A. Gil, Chromium-saponite clay catalysts: Preparation, characterization and catalytic performance in propene oxidation. Copyright (2007), with permission from Elsevier.

of a $(CH_3)_2SnCl_2$ solution (Fig. 7). The spectrum of the intercalated clay was similar to that of a frozen solution of the Sn-trimer and displayed a broad symmetric doublet that could be fitted with two symmetry doublets with an area of 2:1, compatible with the Sn-trimer, which has two terminal and equivalent Sn atoms, and one central Sn atom. When the intercalated clay was heated in the 100–150 °C range, the spectra remained identical, but a dramatic change occurred when heating was carried out at ≥200 °C. The solids thus obtained showed three doublets, one of them showing the isomer shift and quadrupole splitting characteristic of SnO_2. This doublet increased at the expense of the other two when the calcination temperature increased. This indicated that the trimeric species were maintained in the interlayer space up to 200 °C, but that they gradually disintegrate at higher temperature, with the progressive formation of SnO_2; some of this SnO_2 migrates out of the clay interlayer space but part of it keeps the layers apart up to 300 °C.

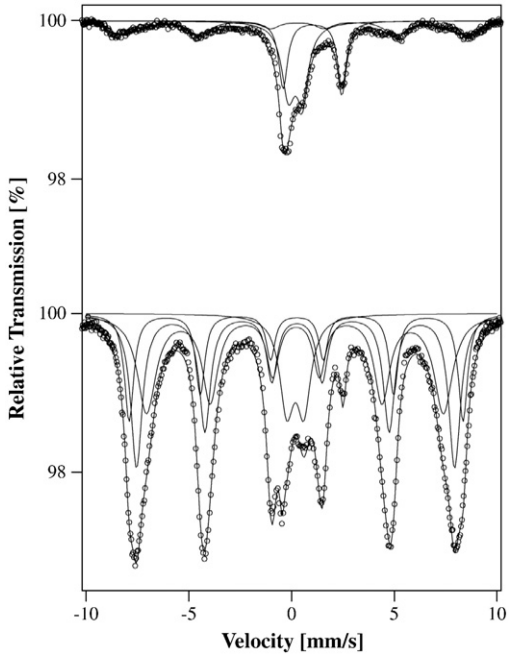

Fig. 6. ^{57}Fe Mössbauer spectra at −268.9 °C of Na-Ballarat saponite (top) and this clay intercalated with Fe_8-tacn polycations (bottom).
Reprinted from Journal of Physics and Chemistry of Solids, 67, L. Stievano, K. Mbemba, C. Train, F.E. Wagner, J.-F. Lambert, Intercalation of $[Fe_8(\mu_3\text{-}O)_2(\mu_2\text{-}OH)_{12}(tacn)_6]^{8+}$ single molecule magnets in saponite clay. Copyright (2006), with permission from Elsevier.

2.5. Thermogravimetry and Differential Thermal Analysis (TGA and DTA)

As indicated in the Introduction, calcination at a moderate temperature is a key step in the preparation of pillared clays, since in this step the metastable polyoxocations are transformed into stable pillars. In a first approach, this step is a simple dehydration, which in the case of Al_{13}-Keggin-like polycations, the most used and best known, may be described by the following equation:

$$[Al_{13}O_4(OH)_{24}(H_2O)_{12}]^{7+} \rightarrow 6.5Al_2O_3 + 20.5H_2O + 7H^+$$

This equation suffices for an idea of what is actually happening in the solid during heating, although this is a very simple approximation because the pillars are not simple metal oxides and because during this process the cross-linking reaction also takes place, which involves the formation of true bonds between the pillars and clay mineral layers. Similar equations may be written for the transformation of polymeric species such as $[Ga_{13}O_4(OH)_{24}(H_2O)_{12}]^{7+}$, $Zr_4(OH)_8(H_2O)_{16}]^{8+}$ or $[(TiO)_8(OH)_{12}]^{4+}$ into Ga_2O_3, ZrO_2 and TiO_2, respectively. The heating of Al-, Ti- and Zr-intercalated clays is usually carried out under an air atmosphere, and it is evident that the same results would be expected if their heating is carried out under inert atmosphere. However, this may not be the case of the calcination of Cr- or Fe-intercalated clays, in which different transformations can be observed under inert or oxidant atmospheres.

Vicente et al. (2001a,b) have reported the TGA and DTA behavior of a saponite intercalated with Al-, Cr-, Al/Cr-, Zr-, and Ti-polycations when heated under controlled atmospheres of air and nitrogen. In the case of Al-PILCs, the results were found to be independent of the atmosphere used while heating. Only small differences in mass loss were observed between raw clay minerals and Cr-, Al/Cr-, Zr-PILCs. The mass loss was slightly higher in the case of Ti-polycations-PILC. The thermal curves of Al–Fe pillared saponite, with different Al/Fe ratios, showed similar behavior for all the solids, but with a significant increase in mass loss with the enhancement in the Fe fraction in the intercalating solutions. The solids intercalated with pure Al- and pure Fe-polycations showed 17 and 21% mass losses respectively, and intermediate values were observed for the solids intercalated with mixed polycations (Belver et al., 2004a).

Vicente et al. (2001a,b) have also reported an interesting effect of the intercalating species in the high-temperature (800–900 °C) transformation from saponite to enstatite and silica or from montmorillonite to mullite and silica. The presence of intercalating species leads these transformations to occur at higher temperatures in the intercalated solids than in raw clay minerals, the typical effects associated with these transformations even completely disappearing.

TGA–DTA may be even more informative when clay minerals are intercalated with polycations containing organic moieties. In this case, the decomposition of the polycations may be very different under inert or oxidizing atmospheres; the latter must be used if a complete transformation of the polycations into pillars without generating carbonaceous deposits is desired. Only a few examples of polycations containing organic moieties can be found in the literature. For example, Vicente and Lambert (1999) reported the thermal treatment of the previously mentioned Ballarat saponite intercalated with Al_{13}-heidi polycations. At low temperature, below 200 °C, the removal of water, either physisorbed or bound to the pillars, is observed, with a

mass loss of c.a. 20% associated with a strong endothermal effect. Between 300 and 380 °C, a mass loss of 7% was found when the analyses were carried out in an air atmosphere, associated with a strong exothermal effect, this being assigned to the combustion of the heidi ligands; this combustion was complete since no carbonaceous residue was observed. The process was similar under a nitrogen atmosphere, the exothermal effect being less intense. However, in this case, the final solids were black, which suggests that the second effect is actually a kind of pyrolysis. Thus, the most important conclusion was that under an air atmosphere, the decomposition of the organic moieties was completed at c.a. 380 °C.

Another example of a polycation containing organic moieties with a perfectly detailed formula and structure is the one mentioned earlier: $[Fe_8(\mu_3\text{-}O)_2(\mu_2\text{-}OH)_{12}(tacn)_6]^{8+}$. Unfortunately, Stievano et al. (2006) did not report the Thermal Analysis of the solids obtained by intercalation of this cation in saponite. Additionally, the thermal analyses of solids containing polycations with unknown formulas have been reported. For example, Toranzo et al. (1998) reported the TGA and Differential Scanning Calorimetry (DSC) of several clay minerals intercalated with a commercial solution containing zirconium–acetic acid species (Fig. 8). This solution affords to pillared solids with excellent properties, obtained under much softer conditions as compared with the traditional pillaring of zirconium oxychloride, which must be carried out in very acidic medium. The curve obtained in the case of Ballarat saponite clearly shows the presence of acetate groups coordinating Zr(IV) cations; these acetate groups decompose below 400 °C, leading to ZrO_2-like pillars. In the case of titanium, several alkoxides have been used as pillaring precursors, and their decomposition to form TiO_2-like pillars has also been studied in thermal analyses (e.g., Vicente et al., 2001a,b).

2.6. Temperature Programmed Reduction (TPR)

Many impregnated catalysts have been prepared by using pillared clays as supports and impregnating them with precursors containing cations of Pt, Pd, Cu, Ni, Fe, V, Cr, Mn, and Co, among other elements. The reducibility of the catalysts thus prepared has been reported by many authors. In the same sense, some of the elements used for doping PILCs are also reducible, and doped PILCs have also been studied by TPR. It is evident that in these cases it is not the behavior of PILCs being studied but that of the solids derived from them, and that the reducibility is due to the impregnating or doping species. Thus, the only reducible cations that form pillared clays are Fe^{3+} and Cr^{3+}.

Belver et al. (2004a) have reported the TPR behavior of several mixed Al–Fe-PILCs, prepared from solutions containing various Al/Fe ratios (Fig. 9). All the samples showed several reduction effects, which may be assigned to the reduction of Fe cations in several steps or to the reduction of cations located in several environments. An effect was observed close to 400 °C, with a hydrogen consumption close to $H_2/Fe = 0.5$, and similar to the curve obtained with pure Fe_2O_3, which is why it can be ascribed to the Fe(III) → Fe(II) reduction of easily accessible trivalent cations. An effect observed at higher temperature was ascribed to the reduction of less accessible Fe(III) ions. Thus, a portion of the Fe fixed during the intercalation may form phases that are highly refractive to reduction. It was remarkable that the temperature of the reduction effects decreased when the amount of Fe increased. This was tentatively explained by the formation during the calcination process of Al–Fe mixed oxides (maghemite or spinel-like phases), thanks to the vicinity of Fe and Al in the intercalating species, whose amount may increase with the amount of Fe in the intercalating solutions. In the samples with higher Fe contents, a new effect was observed in the 700–800 °C temperature range, ascribed to the reduction of the Fe^{3+} initially present in the octahedral positions

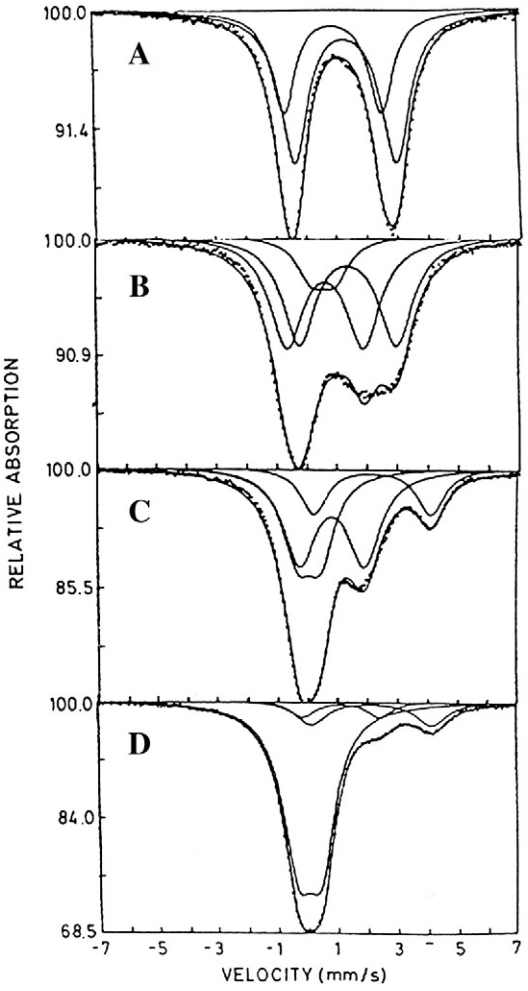

Fig. 7. ^{119}Sn Mössbauer spectra obtained at −196 °C of (A) the intercalated clay and of samples thereof calcined at (B) 200 °C, (C) 250 °C, and (D) 300 °C.
Reprinted with permission from Petridis et al., 1989. Copyright 1989 American Chemical Society.

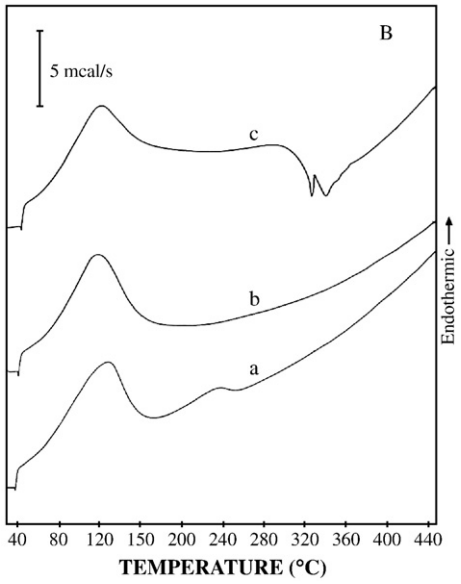

Fig. 8. DSC curves of raw Ballarat saponite (a), the clay intercalated with zirconyl chloride (b) and commercial zirconium acetate solution (c).
Reprinted from Microporous and Mesoporous Materials 24, R. Toranzo, M.A. Vicente, M.A. Bañares-Muñoz, L.M. Gandía, A. Gil, Pillaring of saponite with zirconium oligomers. Copyright (1998), with permission from Elsevier.

of the clay structure. The temperature of the reduction of these cations decreased with the amount of Fe in the solids, suggesting a synergic effect of the new phases on the reduction of the structural clay cations.

The Al–Cr pillared saponite solids reported earlier were also characterized by TPR measurements (Mata et al., 2007). The TPR curves revealed (Fig. 10) that most of the Cr in the solids was in the trivalent state. Its reduction was observed in two processes, the first one centered at 390–400 °C and the second one in a shoulder of this peak at 475 °C. It is well known that the calcination of solids containing chromium under a oxidizing atmosphere produces Cr(VI) species at moderate temperatures, which leads to Cr(III) species when decomposing at higher temperature. Calculations of the amount of hydrogen consumed in the reduction effects showed that all the Cr fixed by the solids was in the form of Cr(VI) when pillaring was carried out by calcination at 400 °C, and that this amount decreased strongly, to values between 5 and 58%, when the pillars were formed by calcination at 500 °C. Additionally, this saponite showed a small reduction effect at high temperature due to the small amounts of Fe(III) located in its octahedral positions.

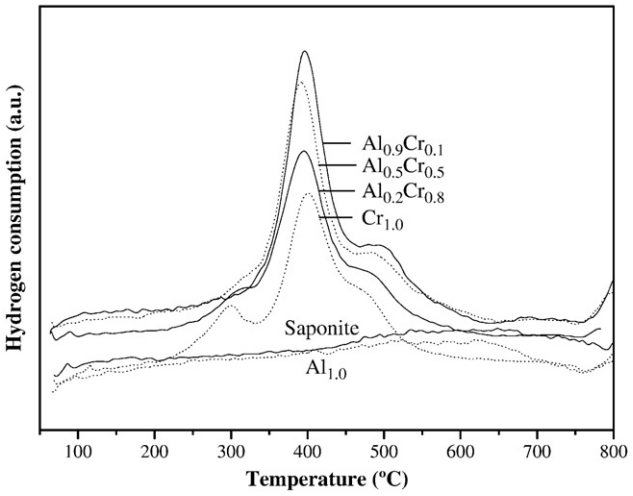

Fig. 10. TPR curves of Al–Cr pillared clays.
Adapted from Applied Catalysis A: General, 327, G. Mata, R. Trujillano, M.A. Vicente, C. Belver, M. Fernández-García, S.A. Korili, A. Gil, Chromium-saponite clay catalysts: Preparation, characterization and catalytic performance in propene oxidation. Copyright (2007), with permission from Elsevier.

2.7. Neutron Scattering (NS)

Neutron Scattering techniques can afford information about some important properties of clay minerals, such as platelet flocculation, particle size or the dynamics of the water in the interlayer region. Pinnavaia et al. (1984) carried out a pioneer work reporting Small-Angle Neutron Scattering (SANS) and Inelastic Neutron Scattering (INS) of some clay mineral samples, including montmorillonite pillared with chlorhydrol. Those authors found a rapid exchange, on the 10^{-9} s timescale, between water molecules at several sites; that is, the behavior of the mobility of water in these clays was more similar to bulk water than to ice, except at certain highly charged sites and when the hydration was higher than that corresponding to the monolayer coverage.

Recently, Chakrabarty et al. (2006) have reported a comparative Quasi-Elastic Neutron Scattering (QENS) study of native and Al_{13}-intercalated saponite. Both samples displayed quasielastic broadening at all the Q values, suggesting the presence of stochastic proton dynamics (Fig. 11). Because the samples dehydrated at 150 °C did not show quasielastic broadening, this suggests an absence of dynamic motion and that the dynamics observed may have been due to adsorbed water molecules. The diffusion constants for the translational motion of adsorbed water molecules were found to be 1.3 $(\pm 0.3)\cdot 10^{-5}$ and 1.75 $(\pm 0.4)\cdot 10^{-5}$ cm^2/s for native saponite and Al_{13}-intercalated saponite, respectively, lower than that of bulk water, while the residence times for translational motion were found to be 4.5 (± 1.0) and 3.6 (± 1.0) ps for native saponite and Al_{13}-intercalated saponite, respectively; higher than that of bulk water. These results reflect a slower motion of water molecules in both saponites than in bulk water, and also show that the mobility of the water adsorbed between the layers of Al_{13}-intercalated saponite is less restricted than the water adsorbed within the interlayers of the native saponite. Comparing both solids, an increase in the basal spacing favors mobility, while the insertion of large polycations into the interlayer region hinders it, and globally the presence of the polycations favors the mobility of water in pillared clays.

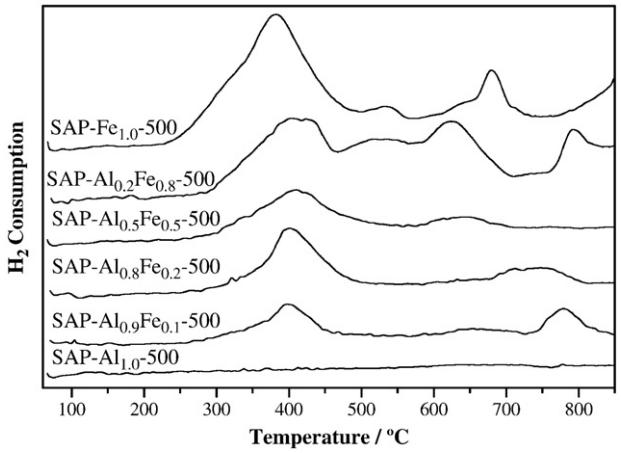

Fig. 9. TPR curves of the Al–Fe pillared clays.
Reprinted from Applied Catalysis B: Environmental, 50, C. Belver, M.A. Bañares, M.A. Vicente, Fe-saponite pillared and impregnated catalysts. I. Preparation and characterisation. Copyright (2004), with permission from Elsevier.

3. Conclusions

The use of specific techniques, other than X-ray diffraction, nitrogen adsorption, infrared spectroscopy and nuclear magnetic resonance, in the characterization of pillared clays offers important information about the properties of these solids. The environment of intercalating cations has been analyzed by visible spectroscopy, while the evolution of the polycations under heating has been followed by Near Infrared Spectroscopy and by Thermogravimetry–Differential Thermal Analysis. The reducibility of the intercalating cations has been followed by Temperature Programmed Reduction, while Electron Paramagnetic Resonance or Mössbauer Spectroscopy has provided important information about the nature of the species formed in the pillared solids, and Neutron Scattering has provided information about the mobility of water in the interlayer region. Although some of these techniques are only useful for certain types of PILCs, they have contributed significantly to structural knowledge about these solids, opening new windows onto the efforts required for new syntheses.

Acknowledgements

The authors thank the financial support from the Spanish Ministry of Science and Innovation (MICINN) and the European Regional Development Fund (FEDER) through project MAT2007-66439-C02.

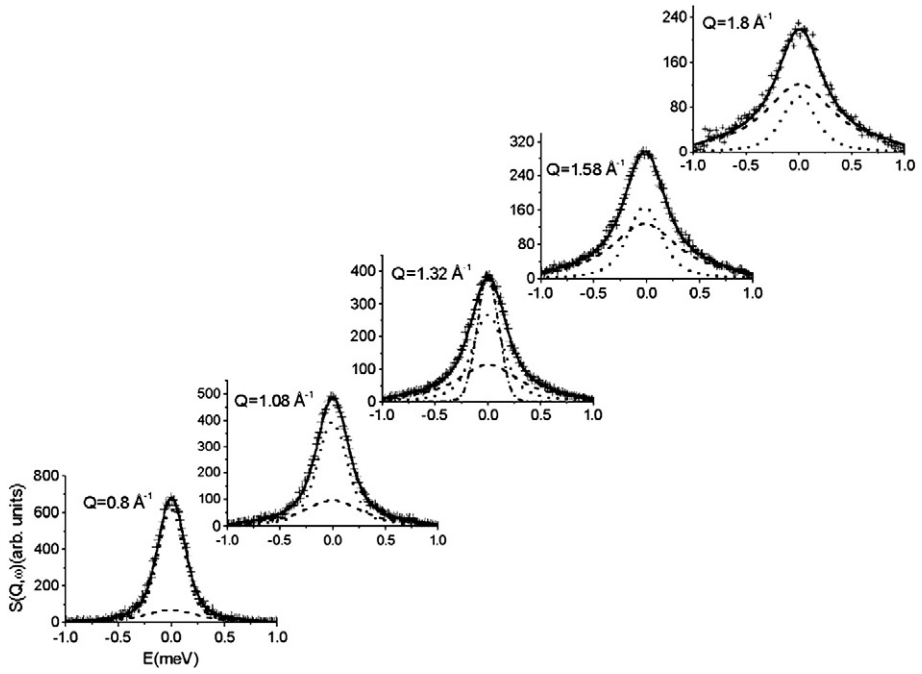

Fig. 11. Fitted QENS spectra at several Q values of water adsorbed in an Al_{13}-intercalated saponite sample considering both rotational and translational motion.
Reprinted from Chemical Physics Letters, 426, D. Chakrabarty, S. Gautam, S. Mitra, A. Gil, M.A. Vicente, R. Mukhopadhyay, Dynamics of absorbed water in saponite clay: neutron scattering study. Copyright (2006), with permission from Elsevier.

References

Bakas, T., Moukarika, A., Papaefthymiou, V., Ladavos, A., 1994. Redox treatment of an Fe/Al pillared montmorillonite. A Mössbauer study. Clays Clay Miner. 42, 634–642.

Belver, C., Bañares, M.A., Vicente, M.A., 2004a. Fe-saponite pillared and impregnated catalysts. I. Preparation and characterisation. Appl. Catal. B 50, 101–112.

Belver, C., Vicente, M.A., Martínez-Arias, A., Fernández-García, M., 2004b. Fe-saponite pillared and impregnated catalysts. II. Nature of the iron species active for the reduction of NOx with propene. Appl. Catal. B 50, 227–234.

Bergaya, F., Aouad, A., Mandalia, T., 2006. Pillared clays. In: Bergaya, F., Theng, B.K.G., Lagaly, G. (Eds.), Handbook of Clay Science. Elsevier, Amsterdam, pp. 393–422.

Brindley, G.W., Yamanaka, S., 1979. A study of hydroxy-chromium montmorillonites and the form of the hydroxy-chromium polymers. Am. Mineral. 64, 830–835.

Chakrabarty, D., Gautam, S., Mitra, S., Gil, A., Vicente, M.A., Mukhopadhyay, R., 2006. Dynamics of absorbed water in saponite clay: neutron scattering study. Chem. Phys. Lett. 426, 296–300.

Ding, Z., Kloprogge, T.J., Frost, R.L., Lu, G.Q., Zhu, H.Y., 2001. Porous clays and pillared clays-based catalysts. Part 2: a review of the catalytic and molecular sieve applications. J. Porous Mater. 8, 273–293.

Finholt, J.E., Thompson, M.E., Connick, R.E., 1981. Hydrolytic polymerization of chromium(III). 2. A trimeric species. Inorg. Chem. 20, 4151–4155.

Gil, A., Gandía, L.M., Vicente, M.A., 2000. Recent advances in the synthesis and catalytic applications of pillared clays. Catal. Rev. 42, 145–212.

Gil, A., Korili, S.A., Vicente, M.A., 2008. Recent advances in the control and characterization of the porous structure of pillared clay catalysts. Catal. Rev. 50, 153–221.

Gil, A., Korili, S.A., Trujillano, R., Vicente, M.A. (Eds.), 2010. Pillared Clays and Related Catalysts. Springer.

Kloprogge, J.T., Duong, L.V., Frost, R.L., 2005. A review of the synthesis and characterisation of pillared clays and related porous materials for cracking of vegetable oils to produce biofuels. Environ. Geol. 47, 967–981.

Mata, G., Trujillano, R., Vicente, M.A., Belver, C., Fernández-García, M., Korili, S.A., Gil, A., 2007. Chromium-saponite clay catalysts: preparation, characterization and catalytic performance in propene oxidation. Appl. Catal. A 327, 1–12.

Petridis, D., Bakas, T., Simopoulos, A., Gangas, N.H.J., 1989. Pillaring of montmorillonite by organotin cationic complexes. Inorg. Chem. 28, 2439–2443.

Pinnavaia, T.J., Rainey, V., Tzou, M.-S., White, J.W., 1984. Characterisation of pillared clays by neutron scattering. J. Mol. Catal. 27, 213–224.

Serwicka, E.M., Bahranowski, K., 2004. Environmental catalysis by tailored materials derived from layered minerals. Catal. Today 90, 85–92.

Spiccia, L., Marty, W., 1986. The fate of "active" chromium hydroxide, $Cr(OH)_3.3H_2O$, in aqueous suspension. Study of the chemical changes involved in its aging. Inorg. Chem. 25, 266–271.

Spiccia, L., Stoeckli-Evans, H., Marty, W., Giovanoli, R., 1987. A new "active" chromium (III) hydroxide: $Cr_2(\mu\text{-}OH)_2(OH)_4(OH_2)_4.2H_2O$. Characterization and use in the preparation of salts of the $(H_2O)_4Cr(\mu\text{-}OH)_2Cr(OH_2)_4^{4+}$ ion. Crystal structure of $[(H_2O)_4Cr(\mu\text{-}OH)_2Cr(OH_2)_4][(H_3C)_3C_6H_2SO_3]4.4H_2O$. Inorg. Chem. 26, 474–482.

Spiccia, L., Marty, W., Giovanoli, R., 1988. Hydrolytic trimer of chromium (III). Synthesis through chromite cleavage and use in the preparation of the "active" trimer hydroxide. Inorg. Chem. 27, 2660–2666.

Stievano, L., Mbemba, K., Train, C., Wagner, F.E., Lambert, J.-F., 2006. Intercalation of $[Fe_8(\mu_3\text{-}O)_2(\mu_2\text{-}OH)_{12}(tacn)_6]^{8+}$ single molecule magnets in saponite clay. J. Phys. Chem. Solids 67, 1363–1371.

Stünzi, H., Marty, W., 1983. Early stage of the hydrolysis of chromium(III) in aqueous solution. 1. Characterization of a tetrameric species. Inorg. Chem. 22, 2145–2150.

Thompson, M., Connick, R.E., 1981. Hydrolytic polymerization of chromium(III). 1. Two dimeric species. Inorg. Chem. 20, 2279–2285.

Toranzo, R., Vicente, M.A., Bañares-Muñoz, M.A., 1997. Pillaring of saponite with aluminum–chromium oligomers. Characterization of the solids obtained. Chem. Mater. 9, 1829–1836.

Toranzo, R., Vicente, M.A., Bañares-Muñoz, M.A., Gandía, L.M., Gil, A., 1998. Pillaring of saponite with zirconium oligomers. Microporous Mesoporous Mater. 24, 173–188.

Vicente, M.A., Lambert, J.-F., 1999. Al-pillared saponites. Part 4. Pillaring with a new Al_{13} oligomer containing organic ligands. Phys. Chem. Chem. Phys. 1, 1633–1639.

Vicente, M.A., Lambert, J.-F., 2001. Synthesis of Pt pillared clay nanocomposite catalysts from $[Pt^{II}(NH_3)_4]Cl_2$ precursor. Phys. Chem. Chem. Phys. 3, 4843–4852.

Vicente, M.A., Toranzo, R., Bañares-Muñoz, M.A., Rodríguez, E., 1998. Diffuse reflectance spectroscopy study of the solids obtained by pillaring of saponite with mixed Al–Cr polycations. An. Quim. 94, 136–141.

Vicente, M.A., Bañares-Muñoz, M.A., Gandía, L.M., Gil, A., 2001a. On the structural changes of a saponite intercalated with various polycations under thermal treatments. Appl. Catal. A 217, 191–204.

Vicente, M.A., Bañares-Muñoz, M.A., Toranzo, R., Gandía, L.M., Gil, A., 2001b. Influence of the Ti precursor on the properties of Ti-pillared smectites. Clay Miner. 36, 125–138.

Vicente, M.A., Belver, C., Trujillano, R., Rives, V., Álvarez, A.C., Lambert, J.-F., Korili, S.A., Gandía, L.M., Gil, A., 2004. Preparation and characterization of Mn- and Co-supported catalysts derived from Al-pillared clays and Mn and Co-complexes. Appl. Catal. A 267, 47–58.

Volzone, C., 1995. Hydroxy-chromium smectite: influence of Cr added. Clays Clay Miner. 43, 377–382.

Volzone, C., 2001. Pillaring of different smectite members by chromium species (Cr-PILCs). Microporous Mesoporous Mater. 49, 197–202.

Volzone, C., Cesio, A.M., Torres Sánchez, R.M., Pereira, E., 1993. Hydroxy-chromium smectite. Clays Clay Miner. 41, 702–706.